

캡슐에 고정화된 흡착제에의 *Berberine*의 흡착에 관한 수학적 모델

† 최 정 우 · 조 상 원 · 이 원 홍

서강대학교 화학공학과

Mathematical Model for Adsorption of Berberine on Encapsulated Adsorbent

Jeong-Woo Choi,† Sang-Won Cho and Won-Hong Lee

Dept. of Chem. Eng., Sogang Univ., C. P. O. BOX 1142, Seoul 100-611, Korea

ABSTRACT

A mathematical model using local thermodynamic equilibrium isotherms for adsorption in encapsulated adsorbent is proposed in order to optimize the design parameters in *in situ* bioproduct separation process. The model accurately follows the experimental data on the adsorption of berberine, secondary metabolite produced in *Thaictum rugosum* plant cell culture. The adsorption rate on encapsulated adsorbent is compared with that on alginate-entrapped adsorbent. The result shows that the higher loading capacity in encapsulated adsorbent is mainly due to the increase in the maximum solid phase concentration. Based on the adsorption rate and loading capacity, the encapsulated adsorbent would be more useful than the entrapped adsorbent when used in *in situ* bioproduct separation process. Design parameters in *in situ* bioproduct separation process, such as the size of the capsule, membrane thickness, the ratio of capsule volume to bulk volume, the ratio of single capsule volume to total capsule volume and the adsorbent content in the capsule, are evaluated by using the model. The ratio of single capsule volume to total capsule volume is the most effective parameter for adsorption of berberine on encapsulated adsorbent.

INTRODUCTION

To enhance process economics through improvements in the primary recovery stages, it is necessary to develop a separation technique which can concentrate the bioproduct, often with some degree of selectivity for the product of interest, and be economical from both capital and operation cost standpoints in large scale cell cul-

ture. In addition to the above mentioned advantages, product separation can enhance the production of secondary metabolites by removing feedback regulation mechanisms and nonspecific inhibitors in plant cell culture (1, 2). For *in situ* product separation of plant cell culture, liquid-solid culture systems for plant cells consisting of an aqueous nutrient phase and of solid polar adsorbents, have been preferred because many products of plant cells are expected to be of polar character and bound weakly to the lipophilic

† Corresponding Author

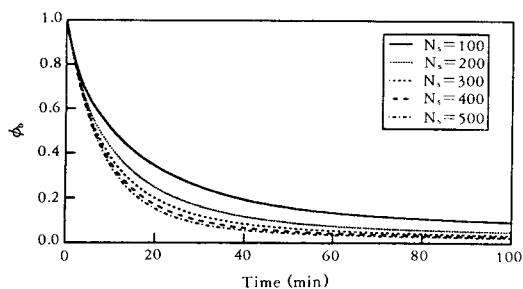


Fig. 9. Simulated bulk concentration profiles for the adsorption of berberine on encapsulated adsorbent by changing the adsorbent content in capsule.

small number of capsules or small size and large number of capsules. It is found that the lower N_c is, the higher the adsorption rate of berberine is. The adsorption rate and capacity of berberine on encapsulated adsorbents are significantly affected by this ratio.

By increasing the adsorbent contents per capsule, N_s , amount of adsorbent used per unit volume of culture medium can be increased with enhancing the binding capacity of beads. Fig. 9 shows the simulation curves indicating the effect of adsorbent content on the adsorption kinetics. The larger value N_s implies the increase of the overall adsorption. However, at very large N_s extent of the effect of N_s on adsorption kinetics decreases. In terms of magnitude, the amount of increase is slightly lower compared to the previous strategies of changing R_0 , N_R and N_c . The value of N_s can be increased only up to a certain limit because mechanical strength of bead decreases and operational difficulty increases in manufacturing increases as N_s increases.

Fig. 10 shows a comparison of the effects of the above design parameters, changing two fold than those in control condition. Adsorption curves for the R_0 , R_m , N_R , N_c and N_s are (b), (c), (d), (e) and (f), respectively, compared to the control condition (a). The adsorption kinetic of berberine is enhanced by using every strategies in terms of rate and the capacity compare to the control

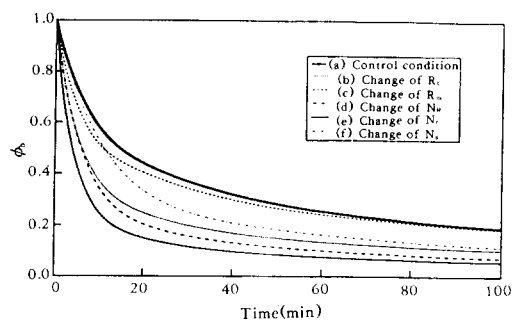


Fig. 10. Simulated bulk concentration profiles for the effect of design parameters when two-fold increased on the adsorption of berberine on encapsulated adsorbent.

case. The highest increase of adsorption rate and capacity is observed by decreasing the ratio of single capsule to total capsule volume (N_c). This result suggests that this ratio is the most effective parameter for adsorption of berberine in encapsulated adsorbent.

Thus, the proposed mathematical model for encapsulated adsorbent can be used for an optimal design on bioproduct separation by evaluating the design parameters. Since the optimization of design parameters depends on specific process condition, it is relatively difficult to achieve an optimal design based on purely empirical correlations. The proposed mathematical model can evaluate the design parameters in various process conditions. When there are one or more compounds present in the fermentation broth which may compete for the adsorption site in the adsorbent particle, the proposed model can be used to evaluate the design parameters to maximize the selectivity of desired product by introducing the index i into the governing equation for each component and adsorption isotherms of various products.

ACKNOWLEDGEMENT

This work was supported by Korea Science and Engineering Foundation, 1992. (Grant No.: 921-1000-009-2)

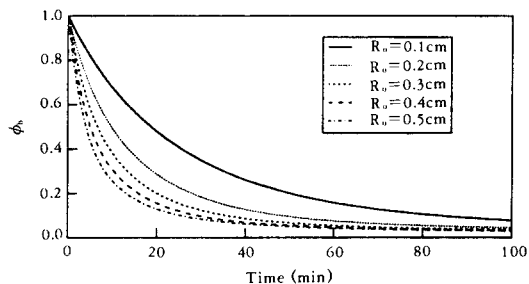


Fig. 5. Simulated bulk concentration profiles for the adsorption of berberine on encapsulated adsorbent by changing the capsule size.

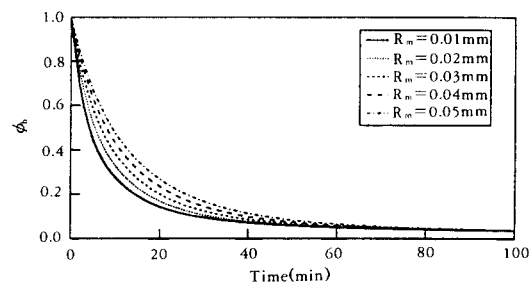


Fig. 6. Simulated bulk concentration profiles for the adsorption of berberine on encapsulated adsorbent by changing the membrane thickness of capsule.

ever, in the practical design the size of bead can be increased only upon a certain limit because the loading number of adsorbent particles increases as bead size decreases and too large beads are difficult to handle and to be separated from culture medium. The optimization of bead size will depend upon specific size of adsorbent and process conditions.

The ratio of capsule radius to core radius is another design parameter, which determines the thickness of the capsule membrane, R_m . Membrane thickness could be controlled by the reaction time with the poly-L-lysine solution. Fig. 6 shows the effect of the membrane thickness on adsorption of berberine. There is not a noticeable change in the equilibrium value for adsorption.

To increase the amount of encapsulated adsorbent used per unit volume of culture medi-

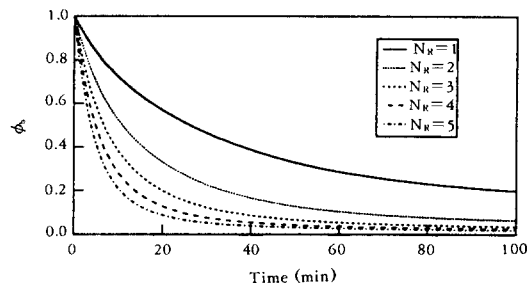


Fig. 7. Simulated bulk concentration profiles for the adsorption of berberine on encapsulated adsorbent by changing the ratio of capsule volume to bulk volume.

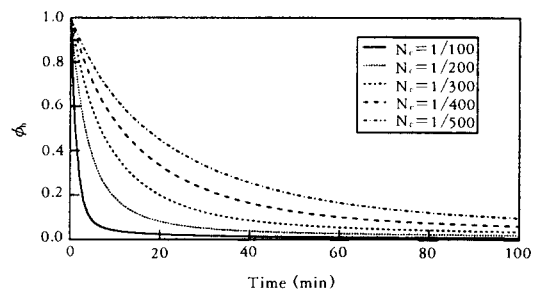


Fig. 8. Simulated bulk concentration profiles for the adsorption of berberine on encapsulated adsorbent by changing the ratio of single capsule volume to total capsule volume.

um can enhance the adsorption kinetics. Fig. 7 shows the simulation curves indicating the effect of changing the volume ratio of capsule to bulk solution, N_R , on the adsorption kinetics. The larger value N_R implies the increase of adsorption at the equilibrium. However, as N_R increases, extent of the effect of N_R on adsorption kinetics decreases. The value of N_R can be increased only up to a certain limit due to maintain appropriate processing conditions and concentration factors.

The effect of the ratio of single capsule volume to total capsule volume, N_t , is simulated as shown in Fig. 8. The ratio of single capsule volume to total capsule volume means the design problem to make the capsules with either large size and

Table 2. Estimated diffusivity and adsorption parameters for the adsorption of berberine on encapsulated and entrapped adsorbent.

| Parameter | Entrapped adsorbent | Encapsulated adsorbent |
|------------------------------|---------------------|------------------------|
| $C_m(\text{mg}/\text{cm}^2)$ | 1.468E-6 | 2.518E-6 |
| $K_s(\text{mg}/\ell)$ | 3.517 | 9.719 |
| $D(\text{cm}^2/\text{min})$ | 4.107E-5 | 5.190E-5 |

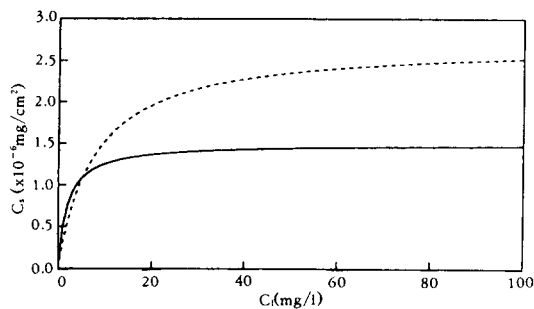


Fig. 4. Adsorption isotherms for the solid (surface) and local liquid (pore) concentrations on encapsulated adsorbent (broken line) and entrapped adsorbent (line).

with the estimated solid (pore) phase and local liquid (surface) phase concentration in entrapped and encapsulated adsorbent. Though the effective diffusivity in entrapped adsorbent particle increases about 26% compared to that in entrapped adsorbent particle based the estimated parameters, the maximum solid phase concentration increases about 72%. The reason for this might be that surface of adsorbents is activated by the liquefaction step of core, which desorbs the ions on adsorbent during gelation process. So the higher loading capacity in encapsulated adsorbents are mainly due to the larger value of the maximum solid phase concentration in adsorbent pore compared with that in entrapped adsorbents. Also the effective diffusivity in adsorbent pore of encapsulated adsorbent is larger than that of entrapped adsorbents, which could be considered as another reason of higher adsorption rate of encapsulated adsorbents as well as the higher diffusivity in

capsule core than that in gel matrix of entrapped adsorbents. The decrease of effective diffusivity in entrapped adsorbent might be due to the filling of alginate solution in the pore of adsorbent particle during immobilization process. However the isotherm equilibrium constant of entrapped adsorbent is higher than that of entrapped adsorbent, which might be due to the decrease of affinity during the capsulation process.

These results suggest that the increase of loading capacity and adsorption rate in encapsulated adsorbent is mainly due to the increase of the maximum solid phase concentration on surface and of the effective diffusivity, respectively. Thus, the proposed mathematical model for encapsulated adsorbent is useful to evaluate the diffusion and adsorption of bioproduct which decide the performance of *in situ* bioproduct separation.

Simulations to Investigate the Effect of Design Parameters

The proposed mathematical model for encapsulated adsorbents can describe various diffusional characteristics in addition to the intrinsic binding characteristics of the encapsulated adsorbents. The performance of encapsulated adsorbent in *in situ* product separation process can be evaluated by using the proposed model for the adsorption rate for target product, berberine in this experiment. The performance of the encapsulated adsorbents is influenced by design parameters such as the capsule size, the membrane thickness, the ratio of capsule volume to bulk volume, the ratio of single capsule volume to total capsule volume and the adsorbent content in the capsule.

The size of capsule, R_0 , can be varied by using a different nozzle or air flow rate during immobilization process. The batches of encapsulated adsorbent beads prepared using this methodology only vary in size but have similar properties of diffusion and adsorption. Fig. 5 shows the simulation curves indicating the effect of capsule size on adsorption kinetics in immobilized adsorbent. The increase in the size of capsule speeds up the binding kinetics significantly. How-

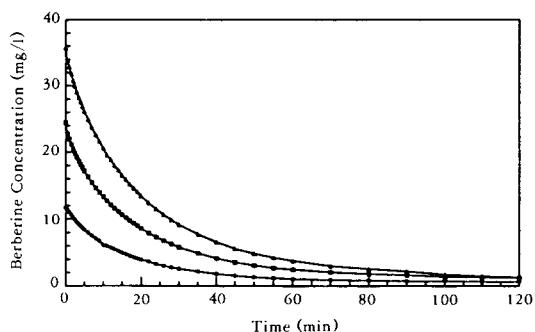


Fig. 2. Experimental (circle) and theoretical (line) results for the adsorption of berberine on encapsulated adsorbent at three different berberine concentration (●: 12mg/l, ■: 24mg/l and ▲: 36mg/l).

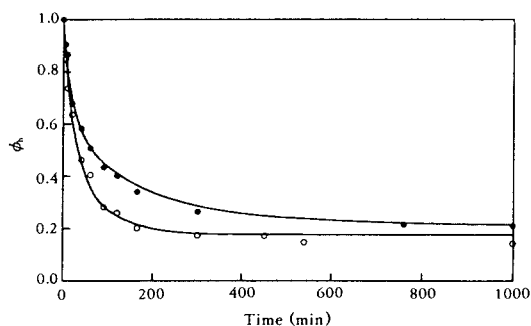


Fig. 3. Experimental (circle) and theoretical (line) results for the adsorption of 140mg/l berberine on encapsulated adsorbent (●) and entrapped adsorbent (○).

The experimental data, C_h vs. θ , are compared to the model predictions by choosing parameters δ , $m\phi_{sm}$ and ω that give a best fit of the model to the data for the adsorption of berberine. A nonlinear parameter estimation technique is used (13, 14) that uses a weighting factor for the residuals proportional to ϕ^{-2} so that the information near equilibrium conditions is highlighted.

RESULTS AND DISCUSSION

Adsorption of Berberine

For the encapsulated adsorbent, the experimental concentration - time curves for berberine

Table 1. Experimental values in simulation for the adsorption of berberine on encapsulated adsorbent.

| | |
|------------------------------|-----------------------------------|
| $\epsilon_s=0.532$ | $a_s=445\text{m}^2/\text{gXAD-7}$ |
| $r_o=2.25\text{mm}$ | $R_o=1.991\text{E-}1\text{cm}$ |
| $R_m=3.5\text{E-}3\text{cm}$ | $V_b=100\text{ml}$ |
| $n=426$ | $N_o=398$ |

adsorption are shown in Fig. 2 for three different initial berberine concentrations within low concentration (less than 100mg/l). As the berberine concentration increases, the adsorption rate increases but the equilibrium value is the same due to the high loading capacity of resin.

For the encapsulated and entrapped adsorbent, the experimental concentration-time curves for berberine adsorption are shown in Fig. 3 for high initial berberine concentrations. Table 1 shows the experimental values to be used for simulation. Void fraction, ϵ_s , and available surface area, a_s , for XAD-7 was reported by Paleos (15). In reference 15, the hydrophobic property of XAD-7 was also reported. The experimental data shown were used in the parameter estimation routine to find isotherm parameters and diffusivity coefficient of berberine in the adsorbent particle, which decide the loading capacity in encapsulated adsorbents. For the entrapped adsorbent, the same technique is used in reference 10. The model results with these estimates are shown as smooth, solid curve in Fig. 3. It is seen that the model is quite consistent and is able to approximate all the experimental data fairly well. The corresponding estimates of parameters are shown in Table 2. The result shows that the amount of berberine adsorbed on encapsulated adsorbents is apparently larger than that on entrapped adsorbent and adsorption rate of the encapsulated adsorbent is apparently higher than that of entrapped adsorbent. Thus, based on the adsorption rate and loading capacity, the encapsulated adsorbent would be more useful than the entrapped adsorbent when used in *in situ* bioproduct separation process.

Fig. 4 shows the adsorption isotherm curve

be approximations to the corresponding derivatives at the location ξ that are the roots of an Nth-order Jacobi polynomial. The semidiscretization elements $A1_{fg}$, $B1_{fg}$, $A2_{pq}$, $B2_{pq}$, $A3_{uv}$ and $B3_{uv}$ that are used to approximate the first and second derivatives, respectively, depend on particular polynomial used.

The evaluation of these elements and the underlying theoretical support for the method can be found in Villadsen and Michelsen (10) who also provides subroutine listings used in this study. The boundary condition for the adsorbent particle is $\phi_{1,1+1} = \phi_c$, where L is the number of internal collocation points that corresponds to a particular Lth-order polynomial approximation. The boundary condition for capsule core is $\phi_{c,M+1} = \phi_{m,0}$, where M is the number of internal collocation points that corresponds to a particular Mth-order polynomial approximation, and that for hydrogel membrane is $\phi_{m,N+1} = \phi_b$ where N is the number of internal collocation points that corresponds to a particular Nth-order polynomial approximation. Since the boundary condition for the adsorbent and capsule core are coupled and that for capsule core and hydrogel membrane are coupled, the boundary condition can be expressed as $\phi_b = \phi_{m,N+1}$, $\phi_{m,0} = (\phi_{c,M+1})_0 = ((\phi_{1,1+1})_{M+1})_0$. Substituting the above relationships into a diffusion equations yield a set of first-order differential equations. And boundary condition (22) could be also converted into the first-order differential equation (52) by substituting eqs. (41) and (43) into eq. (22).

For adsorbent

$$\frac{d\phi_f}{d\theta} = \frac{\delta}{\Gamma(\phi_f)} \sum_{g=1}^{L+1} E_{fg} \phi_{fg}, f=1 \sim L \quad (46)$$

$$\text{where } E_{fg} = 6A1_{fg} + 4\zeta_f B1_{fg} \quad (47)$$

For capsule core,

$$\frac{d\phi_p}{d\theta} = \frac{d[\phi_{1,1+1}]_p}{d\theta} = \beta \left(\sum_{q=1}^{M-1} F_{pq} \phi_{pq} - 6N_c \delta \sqrt{\beta} \sum_{k=1}^{L-1} A1_{fk} \phi_{fk} \right), \quad (48)$$

$$\text{where } F_{pq} = 6A2_{pq} + 4\xi_p B2_{pq} \quad (49)$$

For capsule membrane,

$$\frac{d\phi_{mv}}{d\theta} = \frac{\beta}{\gamma} \sum_{v=0}^{N+1} G_{uv} \phi_{mv}, u=1 \sim N \quad (50)$$

$$\text{where } G_{uv} = 6A3_{uv} + 4\xi_u B3_{uv} \quad (51)$$

For bulk phase,

$$\frac{d\phi_b}{d\theta} = \frac{d[\phi_{m,N+1}]}{d\theta} = -\frac{6\beta}{\gamma} N_k \sum_{v=0}^{N+1} A3_{uv} \phi_{mv}, \quad (52)$$

$u=0 \sim N$

and, for boundary condition at the interface between membrane and core,

$$\sum_{v=0}^{N+1} A3_{uv} \phi_{mv} = \gamma \sum_{q=1}^{M-1} A2_{M+1,q} \phi_{qp} \quad (53)$$

that are easily integrated by an explicit Runge-Kutta method (10, 11) with the initial conditions $\phi_{1f}(0) = 0$, $\phi_{cp}(0) = 0$, $\phi_{mv}(0) = 0$ and $\phi_b(0) = 1$.

Parameter Estimation

Under the conditions where the relative volumes are known and the diffusion coefficients in capsule core and capsule membrane can be estimated *a priori*, the parameters of single component adsorption to work with are δ , $m\phi_{sm}$ and ω . The diffusion coefficients in capsule core and capsule membrane are estimated by using the method described by Tanaka et al. (12). D_c and D_m for berberine are $5.986 \times 10^{-4} \text{ cm}^2/\text{min}$ and $6.174 \times 10^{-5} \text{ cm}^2/\text{min}$, respectively. Diffusion coefficient in alginate-gel matrix is $2.888 \times 10^{-4} \text{ cm}^2/\text{min}$.

The solution to eqs. (45), (47), (49) (51) and (52) depends on the choice of L, M, N and the Jacobi polynomial used for the basic functions. The Jacobi polynomial used in all numerical approximations is characterized by the weighting factor $\xi^{1/2}(1-\xi)$ over the interval $0 < \xi < 1$ and $\xi'^2(1-\xi')$ over the interval $0 < \xi' < 1$. $L=4$ for the adsorbent particle, $M=4$ for the capsule core and $N=2$ for capsule membrane are chosen as the number of internal collocation points, which represent a compromise between extreme accuracy and computational speed.

$$\left| \frac{\partial \phi_m}{\partial \bar{R}} \right|_{\bar{R}=\bar{R}_c^+} = \gamma_i \left| \frac{\partial \phi_c}{\partial \bar{R}} \right|_{\bar{R}=\bar{R}_c^-} \quad (23)$$

$$|\phi_i|_{\bar{r}=1} = \phi_c \quad (24)$$

$$|\phi_i|_{\bar{R}=1} = 1 \quad (25)$$

The dimensionless variables ϕ are introduced by normalizing the corresponding concentration C to the initial product concentration C_0 . The other dimensionless groups are defined as

$$\theta = \frac{D_i t}{r_0^2} \quad (26)$$

$$\bar{R} = \frac{R}{R_0} \quad (27)$$

$$\bar{R}_c = \frac{R_c}{R_0} \quad (28)$$

$$\bar{r} = \frac{r}{r_0} \quad (29)$$

$$\beta = \frac{r_0^2}{R_0^2} \quad (30)$$

$$\gamma = \frac{D_i}{D_m} \quad (31)$$

$$N_R = \frac{nV_{II}}{V_B} \quad (32)$$

where V_{II} is the total volume of the capsule. The dimensionless group parameters that define the particular problems are

$$\delta = \frac{D_1}{D_c} \quad (33)$$

$$\omega = \frac{K_s}{C_0} \quad (34)$$

$$m \phi_{sm} = m \frac{C_{sm} a_s}{C_0} \quad (35)$$

The parameters to be estimated are D_1 , C_{sm} and K_s . The model is reduced to the functional form $\phi = \phi(\theta; \delta, m\phi_{sm}, \omega)$.

Numerical Techniques

For encapsulated adsorbent, it is convenient to introduce the transformation $\xi = \bar{R}^2$ and $\zeta = \bar{r}^2$ to

eliminate eq. (21) and the two-point nature of the boundary conditions. Thus, the governing equations are further reduced to

$$\frac{d\phi_b}{d\theta} = -\frac{6\beta}{\gamma} N_R \left| \frac{\partial \phi_m}{\partial \xi} \right|_{\xi=1} \quad (36)$$

$$\frac{\partial \phi_m}{\partial \theta} = \frac{\beta}{\gamma} \left[6 \frac{\partial \phi_m}{\partial \xi} + 4 \xi \frac{\partial^2 \phi_m}{\partial \xi^2} \right] \quad (37)$$

$$\frac{\partial \phi_c}{\partial \theta} = \beta \left[6 \frac{\partial \phi_c}{\partial \xi} + 4 \xi \frac{\partial^2 \phi_c}{\partial \xi^2} - 6N_s \delta \sqrt{\beta} \left| \frac{\partial \phi_i}{\partial \zeta} \right|_{\zeta=1} \right] \quad (38)$$

$$\frac{\partial \phi_i}{\partial \theta} = \frac{\delta}{\Gamma(\phi_i)} \left[6 \frac{\partial \phi_i}{\partial \zeta} + 4 \zeta \frac{\partial^2 \phi_i}{\partial \zeta^2} \right] \quad (39)$$

and the initial and boundary conditions given in eqs. (20), (21), (22), (23) and (24). These equations can be solved using the method of orthogonal collocation (10).

For the product concentration in the adsorbent, let

$$\frac{\partial \phi_{1f}}{\partial \zeta} = \sum_{k=1}^{l+1} A l_{1k} \phi_{1k} \quad (40)$$

$$\frac{\partial^2 \phi_{1f}}{\partial \zeta^2} = \sum_{k=1}^{l+1} B l_{1k} \phi_{1k} \quad (41)$$

be approximations to the corresponding derivatives at the location ξ that are the roots of an l -th-order Jacobi polynomial.

For the product concentration in the capsule core, let

$$\frac{\partial \phi_{cp}}{\partial \xi} = \sum_{q=1}^{M+1} A 2_{pq} \phi_{cp} \quad (42)$$

$$\frac{\partial^2 \phi_{cp}}{\partial \xi^2} = \sum_{q=1}^{M+1} B 2_{pq} \phi_{cp} \quad (43)$$

be approximations to the corresponding derivatives at the location ξ that are the roots of an M -th-order Jacobian polynomial.

For the product concentration in the hydrogel membrane, let

$$\frac{\partial \phi_{mu}}{\partial \xi} = \sum_{v=0}^{N+1} A 3_{uv} \phi_{mu} \quad (44)$$

$$\frac{\partial^2 \phi_{mu}}{\partial \xi^2} = \sum_{v=0}^{N+1} B 3_{uv} \phi_{mu} \quad (45)$$

phase and membrane phase, respectively. R_o is the outer radius of the capsule and V_B is the bath volume. D_m is the diffusivity in the membrane and n is the number of capsule.

Mass balance in gel membrane of capsule is given by

$$\frac{\partial C_m}{\partial t} = \frac{D_m}{R^2} \frac{\partial}{\partial R} \left[R^2 \frac{\partial C_m}{\partial R} \right] \quad (2)$$

Volume averaged homogeneous conservation equation for capsule core phase is

$$\frac{\partial C_c}{\partial t} = \frac{D_c}{R^2} \frac{\partial}{\partial R} \left[R^2 \frac{\partial C_c}{\partial R} \right] - \frac{3N_s \gamma_0^2 D_1}{R_0^3} \left. \frac{\partial C_1}{\partial r} \right|_{r=0} \quad (3)$$

where D_c and D_1 are the effective diffusivity in capsule core and adsorbent pore, respectively. And N_s is the number of adsorbent per capsule. C_c and C_1 are the concentration in core phase and liquid (pore) phase of adsorbent, respectively.

Volume averaged homogeneous conservation equation for adsorption in the adsorbent particle is

$$\frac{\partial C_T}{\partial t} = \frac{D_1}{\gamma^2} \frac{\partial}{\partial r} \left[r^2 \frac{\partial C_1}{\partial r} \right] \quad (4)$$

where C_T is the total product concentration in the adsorbent, given by

$$C_T = C_1 + m a_s C_s \quad (5)$$

where C_1 and C_s are the liquid (pore) and solid (surface) concentrations, respectively, and a_s is the solid area available for adsorption. The void fraction is ϵ_s and the parameter m is

$$m = \frac{1 - \epsilon_s}{\epsilon_s} \quad (6)$$

The initial conditions ($t=0$) are

$$C_b = C_{b0} \quad (7)$$

$$C_m = C_c = C_1 = C_s = 0 \quad (8)$$

The associated boundary conditions are

$$\left. \frac{\partial C_c}{\partial R} \right|_{R=0} = \left. \frac{\partial C_1}{\partial r} \right|_{r=0} = 0 \quad (9)$$

$$D_m \left. \frac{\partial C_m}{\partial R} \right|_{R=R_c^+} = D_c \left. \frac{\partial C_c}{\partial R} \right|_{R=R_c^-} \quad (10)$$

$$C_1 = C_c \quad \text{at } r=r_0 \quad (11)$$

$$C_b = C_{b0} \quad \text{at } R=R_o \quad (12)$$

These equations are supplemented by an equilibrium relation for solid-phase and local liquid-phase concentrations. For adsorption isotherm of berberine, Langmuir adsorption isotherm which has been experimentally confirmed is chosen (5).

$$C_s = \frac{C_{sm} \cdot C_1}{K_s + C_1} \quad (13)$$

where C_{sm} is the maximum solid phase concentration in adsorbent and K_s is an adsorption equilibrium constant.

Furthermore, if external diffusion is important, then eq. (9) becomes

$$D_m \left. \frac{\partial C_m}{\partial R} \right|_{R=R_0} = -k_1 (C_m - C_b) \quad (14)$$

where k_1 is the mass transfer coefficient.

In dimensionless form, equations (1)-(4) are reduced to

$$\frac{d\phi_b}{d\theta} = -3 \frac{\beta}{\gamma} N_R \left. \frac{\partial \phi_m}{\partial R} \right|_{R=1} \quad (15)$$

$$\frac{\partial \phi_m}{\partial \theta} = \frac{\beta}{\gamma} \frac{1}{R^2} \frac{\partial}{\partial R} \left[\frac{\partial \phi_m}{\partial R} \right] \quad (16)$$

$$\frac{\partial \phi_c}{\partial \theta} = \beta \left[\frac{1}{R^2} \frac{\partial}{\partial R} \left[R^2 \frac{\partial \phi_c}{\partial R} \right] - 3N_s \delta \sqrt{\beta} \left(\frac{\partial \phi_1}{\partial r} \right)_{r=1} \right] \quad (17)$$

$$\frac{\partial \phi_1}{\partial \theta} = \frac{\delta}{\Gamma(\phi_1)} \frac{1}{r^2} \frac{\partial}{\partial r} \left[\frac{\partial \phi_1}{\partial r} \right] \quad (18)$$

$$\text{where } \Gamma(\phi_1) = 1 + \frac{m\phi_{sm}\omega}{(\omega + \phi_1)^2} \quad (19)$$

The initial conditions become

$$\phi_b = 1 \quad \text{for } \theta = 0 \quad (20)$$

$$\phi_m = \phi_c = \phi_1 = \phi_s = 0 \quad \text{for } \theta = 0 \quad (21)$$

The boundary conditions become

$$\left. \frac{\partial \phi_c}{\partial R} \right|_{R=0} = \left. \frac{\partial \phi_1}{\partial r} \right|_{r=0} = 0 \quad (22)$$

Preparation of Adsorbent

Prior to use, the resins, XAD-7, were soaked in methanol for 24 hour and then washed with 2 liter distilled water. The washed resins were air dried on the filter paper by pulling a vacuum in the filter flask. Sieve the resin through the nylon nets to get suitable size distribution.

Entrapped Adsorbent

XAD-7 was suspended in viscous sodium alginate solution (2% w/w) and the droplets of this solution were fallen into 1.5% (w/w) calcium chloride solution under continuous stirring. The beads were allowed to form for 30 min and then collected by filtration. Beads were washed with distilled water and then were autoclaved in 0.5% CaCl₂ solution to maintain the integrity for 15min at 121°C. The sterilized beads were stored in sterilized water.

Encapsulated Adsorbent

XAD-7 was suspended in viscous sodium alginate solution (2% w/w) and the droplets of this solution were fallen into 1.5% (w/w) calcium chloride solution under continuous stirring. The spherical calcium alginate gel was formed after 5 minutes. The beads were removed and placed in 0.1% (w/v) poly-L-lysine solution for 5 minutes. Semipermeable membrane was formed at the outer surface of beads at this step. The capsules were dropped into 1.5% (w/v) citric acid to liquefy the core for 5 minutes. Then the capsules were stored in distilled water for use.

Adsorber Unit

Slow speed stirring vessel with impeller (Corning Co., Corning, NY) was used as a adsorber unit. The working volumes for encapsulated adsorbent test were 100ml at 180 agitation rpm. Experiments were conducted with dilute aqueous solution of berberine in the adsorber unit. Encapsulated or entrapped resin was added into the adsorber unit. Sample solution was taken from the adsorber unit by the pipet with the cotton filter at various time throughout the experiments.

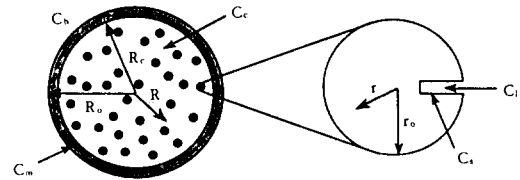


Fig. 1. Schematic diagram of an encapsulated adsorbent.

C_b : Conc. in Bulk Phase

C_m : Conc. in Membrane

C_c : Conc. in Capsule Core

C_i : Conc. in Adsorbent Pore

C_s : Conc. at Adsorbent Surface

R_m : Radius of Capsule Membrane

R_c : Radius of Capsule Core

r : Radius of Adsorbent

Concentrations of berberine was determined by measuring the solution absorbance at 343 nm by spectrophotometer (UV-240, Shimadzu Co, Tokyo). After measuring the UV absorbance of sample solution, the sample solution returned to the adsorber unit. To evaluate diffusivities of berberine in gel, capsule membrane and capsule core, the adsorption experiment was repeated with alginate-gel and capsule in which adsorbents were not contained. All experiments were done at 20°C.

THEORETICAL MODEL

Model Equations

The physical system and the associated notation are depicted in Fig. 1. The assumptions for mathematical model are as follows:

- Adsorbent particle and capsules are sphere.
- Adsorbent particles are distributed uniformly inside the capsule.
- Each diffusivity in the capsule, membrane and adsorbent particles is constant.
- External diffusion of product to capsule is negligible.

Since the bath (bulk) phase is finite, the depletion in bulk phase is

$$\frac{dC_b}{dt} = -\frac{4\pi n R_m^2 D_m}{V_B} \left. \frac{\partial C_m}{\partial R} \right|_{R=R_0} \quad (1)$$

where C_b and C_m are the concentrations in bulk

phase of liquid-liquid systems. The differences in acid-base properties and sorption characteristics of alkaloids further offers the potential for selectively absorbing specific alkaloids from a mixture (3, 4).

Polycarboxylic ester resin, XAD-7, was investigated to adsorb berberine, secondary metabolite from immobilized (alginate-entrapped) *T. rugosum* cells, secreted in permeabilization process and immobilized XAD-7 was developed for *in situ* product separation process in an airlift bioreactor (4, 5). The increases of berberine production in *in situ* separation using suspended, alginate-entrapped-, membrane-entrapped XAD-7 were observed (4, 5). The advantages of immobilized adsorbent were easy to use in bioreactor operation, prevention of surface fouling, and easy separation of adsorbents from cells for the repeated use of cells and adsorbents (4-8). The adsorption of bioproduct on immobilized adsorbent was dependent on a number of design parameters. The performance of the immobilized adsorbent in *in situ* product separation process could be evaluated by judging the adsorption rate for target product. The adsorption behavior of bioproduct was controlled by various diffusional resistances in addition to intrinsic binding characteristics of the free adsorbent particles. Diffusional characteristics were influenced by design parameters such as size of beads, adsorbent content of bead, amount of beads to bulk volume and the type of hydrogel used.

The design and optimization of *in situ* bioproduct separation process using immobilized adsorbent required a detailed mathematical model. Because the effects of various design parameters and process variables were coupled, it was relatively difficult to achieve an optimal design based on purely empirical correlations. In this study, a mathematical model to describe diffusion and adsorption in encapsulated adsorbent is proposed for the evaluation of design parameters on bioproduct separation using encapsulated adsorbents.

Mathematical models for immobilized adsor-

bents have been investigated by using simple Langmuir or Freundlich isotherm and solved by finite difference technique with assumed effective diffusivity of solute in XAD-4 adsorbent for cyclohexamide adsorption system (6) and in DEAE-trisacryl adsorbent for enzyme adsorption system (7). The local thermodynamic equilibrium model could predict the adsorbed enzyme amount in suspended porous supports, Duolite S-761, more accurately than other model (9). Since diffusion through the pores of the carrier or adsorbent occurs far slower than adsorption, the assumption that all points within the carrier or adsorbent remain in local thermodynamic equilibrium can be permitted. Orthogonal collocation technique was clearly superior to solve the equations for adsorption bath or column system than finite difference technique which was found to be stable only for certain parameter values and converged very slowly (9).

In this study, the ability of encapsulated XAD-7 with poly-L-lysine membrane is evaluated for the adsorption of berberine, secondary metabolite of *Thalictrum rugosum* plant cell culture. A mathematical model based on reversible binding with local thermodynamic equilibrium assumptions for the adsorption of bioproduct on encapsulated adsorbents is proposed for quantification of adsorption phenomena and evaluation of the operating parameters. Results of model simulation are compared with experimental data. Design parameters for an optimal design of *in situ* bioproduct separation process are evaluated with the proposed model.

MATERIALS AND METHODS

Materials

Berberine and dopamine were purchased from Sigma Chemical Co. (St. Louis, MO). Calcium chloride was supplied from Osaka chemicals (Osaka, Japan) and the ambertile XAD-7 was obtained from Supelco Inc. (Bellefonte, PA). All other reagents were analytical grade and purchased from Sigma Chemical Co. (St. Louis, MO).

Subscripts

0 initial value

REFERENCES

1. S. E. Skinner, N. J. Walton, R. J. Robins and M. J. C. Rhodes (1987), *Phytochem.*, **26**, 721.
2. G. F. Payne, N. N. Payne, M. L. Shuler and M. Asada (1988), *Biotechnol. Lett.*, **10**, 187.
3. G. F. Payne and M. L. Shuler (1988), *Biotechnol. Bioeng.*, **31**, 922.
4. J. W. Choi (1990), *Ph. D. Thesis*, Dept. of Chem. & Biochem. Eng., Rutgers University, New Jersey.
5. J. W. Choi (1992), *KJChE*, **9**, 128.
6. S. C. Nigam and H. Y. Wang (1986), *Separation, Recovery and Purification in Biotechnology* (J. A. Asenjo and J. Hong, eds) 153, American Chemical Society, Washington D. C.
7. S. C. Nigam (1988), *Ph. D. Thesis*, Dept. of Chem. Eng., University of Michigan, Michigan.
8. S. C. Nigam, A. R. Siahpush and H. Y. Wang (1990), *AIChE J.*, **36**, 1239.
9. H. Pedersen, L. Furler, K. Venkatasubramanian, J. Prenosil and E. Stucker (1985), *Biotechnol. Bioeng.*, **27**, 967.
10. J. V. Villadsen and M. Michelsen (1978), *Solution of Differential Equation Models by Polynomial Approximation*, p. 141, Prentice-Hall, Englewood Cliffs.
11. M. J. Maron (1982), *Numerical Analysis: a Practical Approach*, p. 344, Macmillan Publishing Co., NY.
12. H. Tanaka, M. Matsumura and I. A. Veliky (1984), *Biotechnol. Bioeng.*, **26**, 53.
13. C. M. Metzler, G. L. Elfring and A. J. McEwen (1974), *Biometrics*, **30**, 562.
14. J. Seinfeld and L. Lapidus (1970), *Process Modeling, Estimation and Identification*, p. 383, Prentice-Hall, Englewood Cliffs.
15. J. Paleos (1969), *J. of Colloid and Interface Sci.*, **31**, 7.